Hindawi Publishing Corporation
Physics Research International
Volume 2010, Article ID 120672, 9 pages
doi:10.1155/2010/120672

Research Article

A Comparative Study between the Effects of Magnetic and Nonmagnetic Dopants on the Properties of ZnO Varistors

A. Sedky[1,2] and E. El-Suheel[1]

[1] *Physics Department, Faculty of Science, King Faisal University, P.O. B 400, Al-Hassa 31982, Saudi Arabia*
[2] *Physics Department, Faculty of Science, Assiut University, Assiut 71516, Egypt*

Correspondence should be addressed to A. Sedky, sedky1960@yahoo.com

Received 3 October 2009; Revised 28 December 2009; Accepted 10 February 2010

Academic Editor: Ali Hussain Reshak

A comparative study between effects of Mn and Al on the properties of ZnO varistor sintered at 1200°C is investigated by XRD, SEM hardness, and I-V measurements. Although both Mn and Al do not influence the well-known peaks related to wurtzite structure of ZnO ceramics, some other unknown peaks could be formed at higher doping content (≥ 0.10). Also, the shape and size of grains are clearly different for both dopants. Average crystalline diameters, deduced from XRD analysis, are between 42 nm and 62 nm, which are 50 times lower than those obtained from SEM micrographs, while the oxygen vacancies deduced from EDAX analysis, are gradually decreased by doping content for both dopants. Interestingly, the values of breakdown field, nonlinear coefficient and barrier height are found to be higher in Mn samples as compared to Al samples, while the opposite is reported for leakage currents, hardness, and electrical conductivities. The values of E_B are changed from 2.67 V/cm to 41.67 V/cm for Al, and from 1928 V/cm to 6571 V/cm for Mn. The conductivity of Al samples is higher than that of ZnO, and it is nearly (103–105) times the conductivity of Mn samples. These results are discussed in terms of the difference of magnetic moment and valence state between these two additives.

1. Introduction

Zinc oxide varistor is ceramic semiconductor device with nonlinear current-voltage characteristic. Increase of voltage causes the decrease of resistance, and therefore the current is increased strongly. This nonlinear characteristic is symmetrical and it is the same for both voltage polarities [1]. A typical ZnO-based varistor is a very complex chemical system and contains several oxide additives dopants such as Bi_2O_3, Cr_2O_3, Al_2O_3, MnO, CoO, and Fe_2O_3 [2–5]. The nonlinear current-voltage characteristics of ZnO varistors are directly dependent on the composition and microstructure, such as density, grain size, morphology, and distribution of any second phases. By controlling these parameters, the nonlinearity coefficient and the breakdown field of ZnO varistors may be increased up to 80 and 5000 V/cm, respectively [2].

The charge transfer mainly controls the electrical conduction in ZnO varistors during sintering in oxidizing atmosphere [6–9]. The existence of potential barriers across the grain boundaries of ZnO is confirmed additionally by voltage contrast imaging in the scanning electron microscope (SEM) [10]. At low applied fields, the barrier height is slightly decreased by the field. This is because the electrons capture some increase of the negative interface charge above their absolute value and prevent the sharp barrier lowering. At high field ($\approx$3.2 V) per grain boundary, the barrier height is decreased stronger due to decreasing the negative interface charge than absolute value as a result of holes creation (E_g = 3.2 eV of ZnO) [11]. The appearance of positive charge due to the formation of inversion layer at low fields can lead to the strong increase of the leakage current and helps to explain nonlinear behavior of ZnO varistors [2]. However, the impact of ionization in the depletion region of grains can give sharp decrease of the barrier height even in the case of thermoionic emission [12].

Earlier, we studied the current-voltage characteristic of ZnO samples with Fe as the only magnetic additive and found that samples show significant varistor behavior in both

quenching and slowly cooled samples [13, 14]. The addition of Fe improved the nonlinear properties of ZnO varistor and the electrical barriers could be formed. In the present work, a comparative study between the effects of magnetic (Mn) and nonmagnetic (Al) dopants on the properties of ZnO is investigated.

2. Experimental Details

$Zn_{1-x}M_xO$ samples with various x values ($0.00 \leq x \leq 0.20$ & M = Mn, Al) are synthesized by using conventional solid-state reaction method [13–15]. The powders of ZnO Mn_2O_3 and Al_2O_3 (Aldrich 99.999 purity) are thoroughly mixed in required proportions and calcined at 900°C in air for a period of 12 hours. The resulting powders are ground, mixed, and pressed into disks of 1 cm diameter and 0.3 cm thick. The pellets are then separately sintered at temperatures of 1200°C for 10 hours in air and then quenched down to room temperature. The bulk density of the samples is measured in terms of their weight and volume. The phase purity of the samples is examined by using X-ray diffractometer with Cu-Kα radiation. Microstructure characterization of the samples is studied by scanning electron microscope (SEM). The Vicker microhardness (VHN) of the samples is determined using an MH-6 digital microhardness tester (0.098–9.8 N). The VHN is estimated according to the following equation: $\text{VHN} = 0.1891\,(\text{P}/\text{d}^2)$, where P is the applied load and d is the diagonal length of indenter impression. Finally, I-V characteristics are obtained with an electrometer (model 6517, Keithley), 5 kV dc power supply, and digital multimeter. The samples are well polished and sandwiched between two cupper electrodes and the current is measured relative to the applied voltage at room temperature. High-quality silver paint is used on the samples surfaces for electrical contacts.

3. Results and Discussion

It is noted that the color of pure ZnO and Al doped samples is white while it changed to brown with low doping of Mn content and it becomes brown with higher doping. The bulk densities of the samples, listed in Table 1, are generally decreased by Mn and increased by Al. It is evident from XRD patterns shown in Figures 1(a) and 1(b) that the structure of $Zn_{1-x}M_xO$ samples with $x = 0.00$, 0.025, and 0.05 is Wurtzite structure, and no additional lines could be formed. When x is increased above 0.05, some unidentified peaks denoted by stars could be seen in the XRD pattern of both dopants. Furthermore, the intensity of these lines is increased with increasing doping content. Although the number of these unidentified lines is higher for Mn than Al, the average net intensity is higher for Al than Mn. This is because with increasing doping content above 0.05, the solubility limit of dopants through Zn lattice is reached and some of dopant atoms could be localized at the interstitial position as a secondary lines, as recorded in the XRD patterns. However, the impact of these lines on the nonlinear properties of the considered varistors will be discussed in the next paragraph.

Table 1

(a) Density, leakage currents, and nonlinear coefficients of Al-doped ZnO varistor

Al content	ρ (gm/cm^3)	I_g (A)	α_1	α_3
0.00	5.37	1.51×10^{-4}	2.04	2.09
0.025	6.29	2.46×10^{-4}	0.21	1.63
0.05	6.94	2.97×10^{-4}	0.24	1.43
0.10	5.30	2.82×10^{-4}	0.22	1.47
0.20	4.35	3.01×10^{-4}	0.09	1.61

(b) Density, leakage currents, and nonlinear coefficients of Mn-doped ZnO varistor

Mn content	ρ (gm/cm^3)	I_g (A)	α_1	α_3
0.00	5.37	1.51×10^{-4}	2.04	2.09
0.025	5.16	3.32×10^{-5}	1.45	1.56
0.05	3.88	2.91×10^{-5}	1.28	2.19
0.10	3.76	55.5×10^{-4}	0.51	1.98
0.20	3.77	75.6×10^{-4}	0.34	1.70

To further confirm that both Al^{3+} and $Mn^{3+/4+}$ have been substituted for Zn^{2+} in the cell, are smaller ionic radii of both Al^{3+} (0.51 Å) and $Mn^{3+/4+}$ (0.63 Å), than that of Zn^{2+} (0.74 Å). The average crystalline diameter D_{hkl} is evaluated in terms of X-ray line broadening described by the following Scherer's equation [16]:

$$D_{\text{hkl}} = \frac{k\lambda}{\Delta\theta \cos\theta}, \tag{1}$$

where λ is X-ray wavelength ($\lambda = 1.5418$ Å), $\Delta\theta$ is half maximum line width, θ is Bragg angle, and K is constant ($K = 0.9$ for this type of ceramics). The average values of D_{hkl} versus doping content are shown in Figure 1(b). It is clear that the values of D_{hkl} are increased by 0.025 of doping content followed by a decrease with an increase up to 0.20. The values of D_{hkl} range between 42 nm up to 62 nm for all samples.

The microstructure of pure and doped samples is shown in Figure 2(a). Nearly, no second phases are formed at grain boundaries, but the grains are randomly distributed over the matrix structure. Al content up to 0.10 decreased the average grain size as compared to ZnO sample, and vice versa with higher Al content while Mn generally increased the size of grains. The size of black regions is nearly constant and unaffected by the doping. The average grain size, shown in Figure 2(b), indicates that the size of grains decreased by increasing doping content up to 0.05, followed by an increase up to 0.20 while the size of grains is gradually increased by Mn addition up to 0.20 and it is higher than that of Al samples. The sizes of grains, deduced from SEM micrographs, are between 1610 nm and 3230 nm, which are 50 times higher than those obtained from XRD analysis. Anyhow, it has been reported that diluted magnetic semiconductors are generally formed by partial substitution of n-type ZnO with small amount of transition metals such

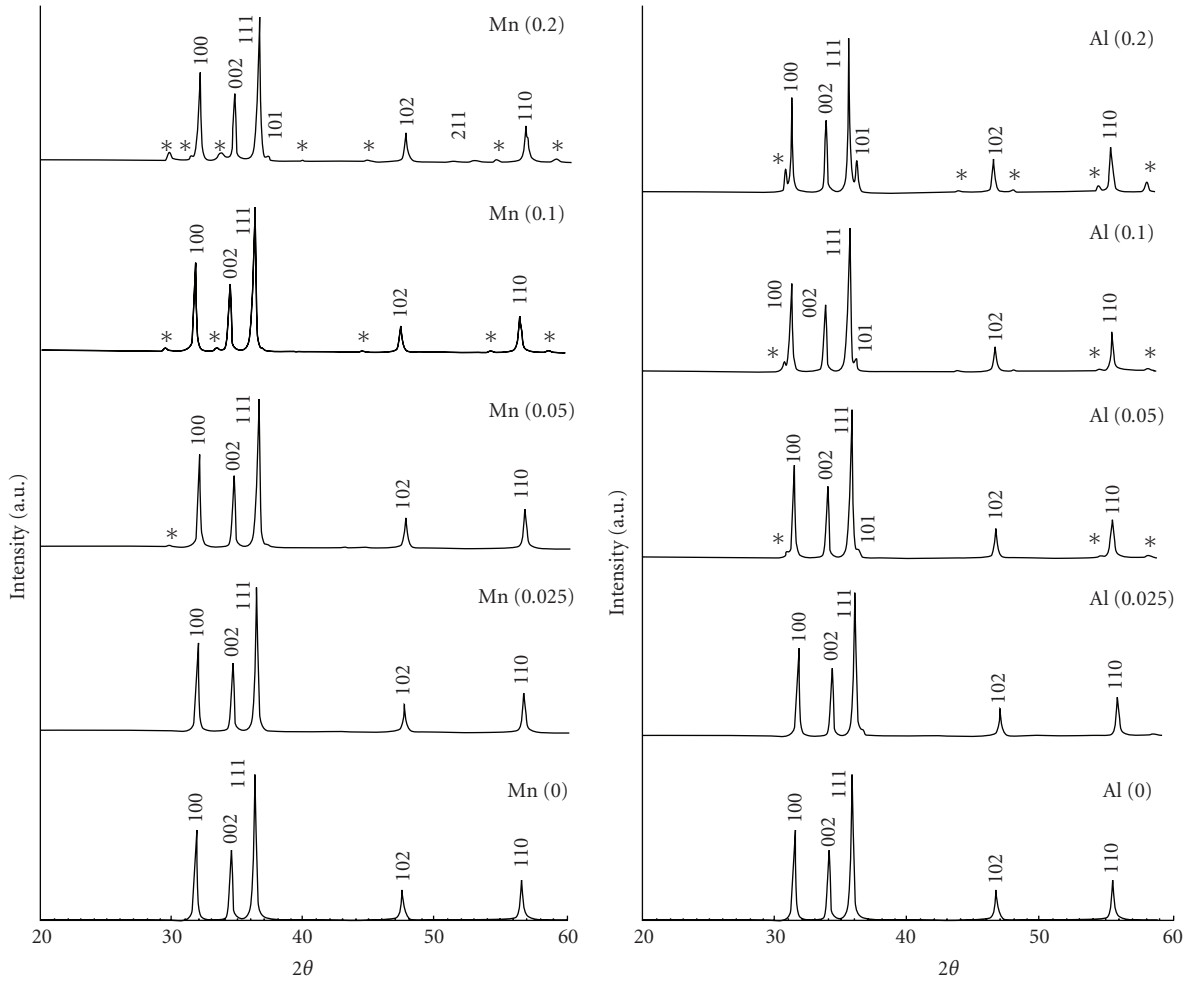

(a)

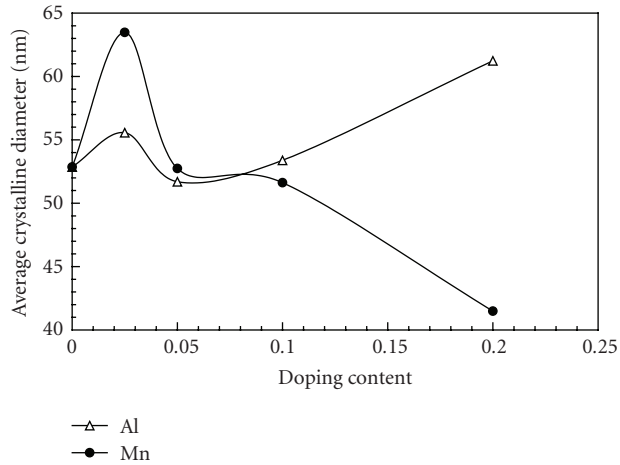

(b)

Figure 1: (a) X-ray diffraction patterns of pure and Mn-doped samples (left) and of pure and Al-doped samples (right). (b) Average crystalline diameter versus doping content for Al and Mn samples.

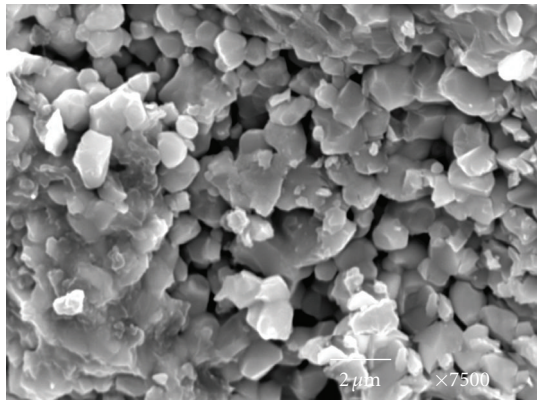

ZnO

(a)

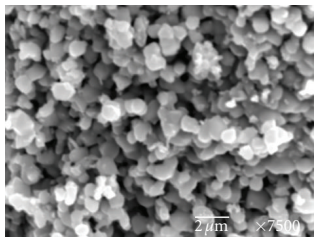

Al1 ($x = 0.025$)

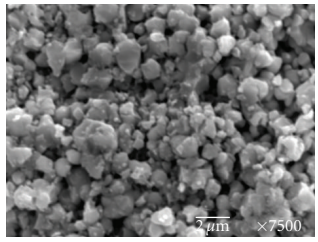

Al2 ($x = 0.05$)

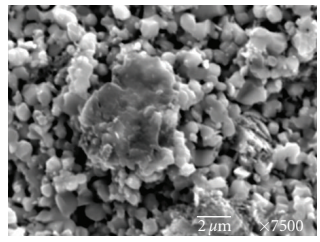

Al3 ($x = 0.1$)

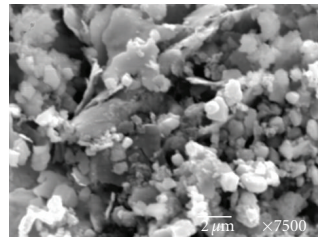

Al4 ($x = 0.2$)

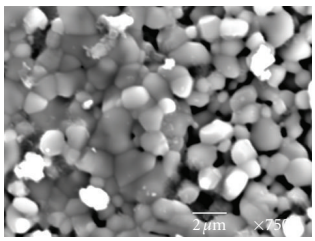

Mn1 ($x = 0.025$)

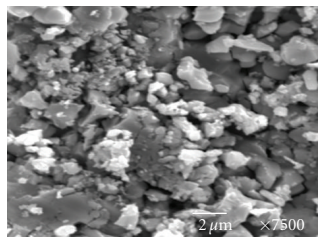

Mn2 ($x = 0.05$)

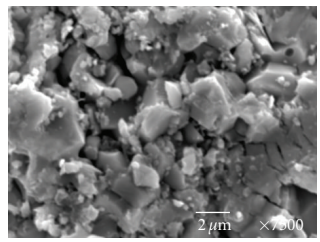

Mn3 ($x = 0.1$)

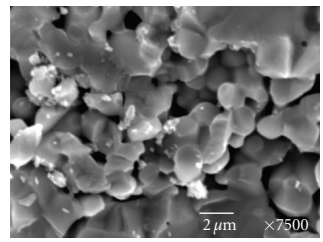

Mn4 ($x = 0.2$)

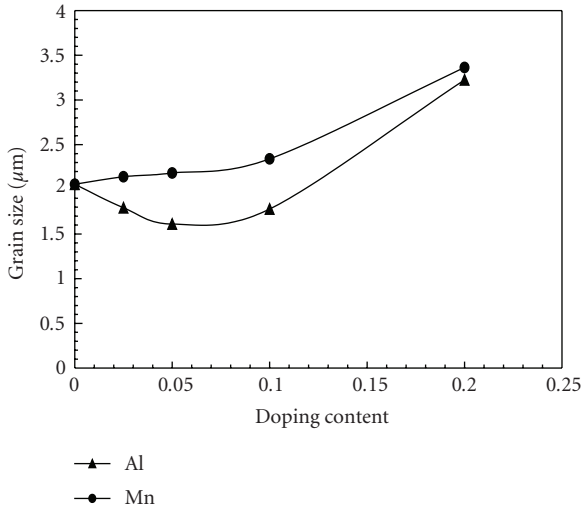

(b)

Figure 2: Continued.

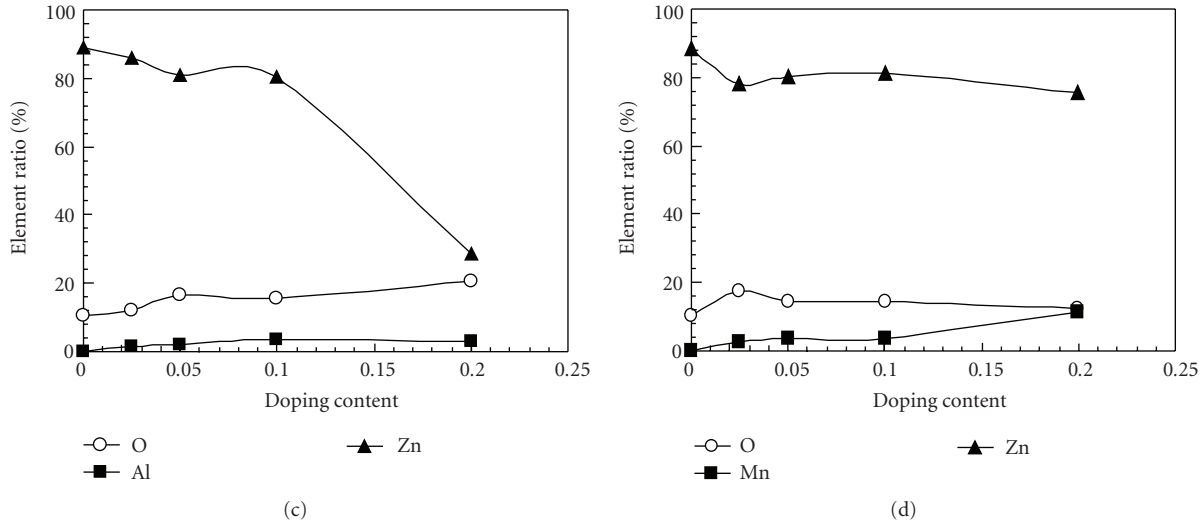

Figure 2: (a) SEM micrographs for pure and doped ZnO samples. (b) Grain size for Pure and Al-doped ZnO samples. (c) Element ratio for Pure and Al doped ZnO samples. (d) Element ratio for Pure and Mn-doped ZnO samples.

as Mn and Ni. In such samples, TEM data show that most of the particles size is around 60 nm [16]. These data support the values of average grain size deduced from XRD analysis rather than those obtained from SEM micrograph. Since HR/SEM and TEM techniques are not available for us at present, this will be taken into consideration for further research. The elements ratio as a function of doping content is shown in Figures 2(b) and 2(c). It is clear that the element ratios of both dopants are decreased while it is slightly increased for oxygen. This means that the oxygen vacancies are slightly decreased by the dopants.

There are three different regions observed in the I-V curves of the samples shown in Figures 3(a) and 3(b). The first and third regions are nearly ohmic behavior, while the other is clearly nonlinear behavior (upturn region). The values of applied fields at the boundary of the nonlinear region are shifted to lower values by Al addition, and vice versa for Mn-doped samples, while the values of current density are generally increased by Al and decreased by Mn. However, the important parameter, E_B, breakdown field is usually taken as the field applied when the current flowing through the varistor is 1 mA/cm^2 [17, 18]. The variation of E_B, obtained from dc electrical measurements, versus doping content is shown in Figure 3(c). It is clear that Al content up to 0.05 decreased E_B, followed by an increase with increasing Al up to 0.20 while E_B is increased by increasing Mn up to 0.20. The highest value of E_B for Mn (6571 V/cm) is approximately 1.5×10^2 times the highest value of E_B for Al (41.67 V/cm). The values of E_B range between 2.67 V/cm and 41.67 V/cm for Al, and it is varied from 1928 V/cm up to 6571 V/cm for Mn. These results indicate that E_B could be increased up to 6571 V/cm by 0.1 of Mn doping, which is higher than that reported for ZnO varistor (5000 V/cm) [2].

The current-voltage relation of a varistor is given by the following equation [17, 18]:

$$J = \left(\frac{E}{C}\right)^{\alpha}, \tag{2}$$

where J is the current density, E is the applied electric field, C is a proportionality constant corresponding to the resistance of ohmic resistor (nonlinear resistance), and α is the nonlinear coefficient. The current-voltage curves are plotted on a log-log scale, from which the slope of the curve gives the value of α [19, 20]. The values of α are obtained across the first and third regions and listed in Table 1, while the variation of α against doping content in the nonlinear region is shown in Figure 3(d). It is apparent that α decreases by Mn doping content up to 0.05, followed by an increase up to 0.20. The values of α are decreased by Al doping and remain lower than the undoped sample, while the values of α at higher doping of Mn doping (0.10 and 0.20) become higher than the undoped sample. From these results, it is determined that the addition of low amount of Al^{3+} oxide to ZnO varistor composition decreased the nonohmic features and shifted the breakdown fields to lower values. while the addition of $Mn^{3+/4+}$ doping generally improved the nonlinear behavior and shifted the breakdown field to higher values. On the other hand, the leakage current I_k is the current value, which corresponds to a field equal to half E_B.These calculations enable us to study the I-V characteristics in the ohmic region as compared to upturn region [1, 6, 21]. When the Al content increases, the low current region goes up and the leakage current, listed in Table 1, slightly increases. The opposite is reported for higher Mn-doped samples. But the increments of the leakage currents are higher in the Al-doped samples than Mn samples.

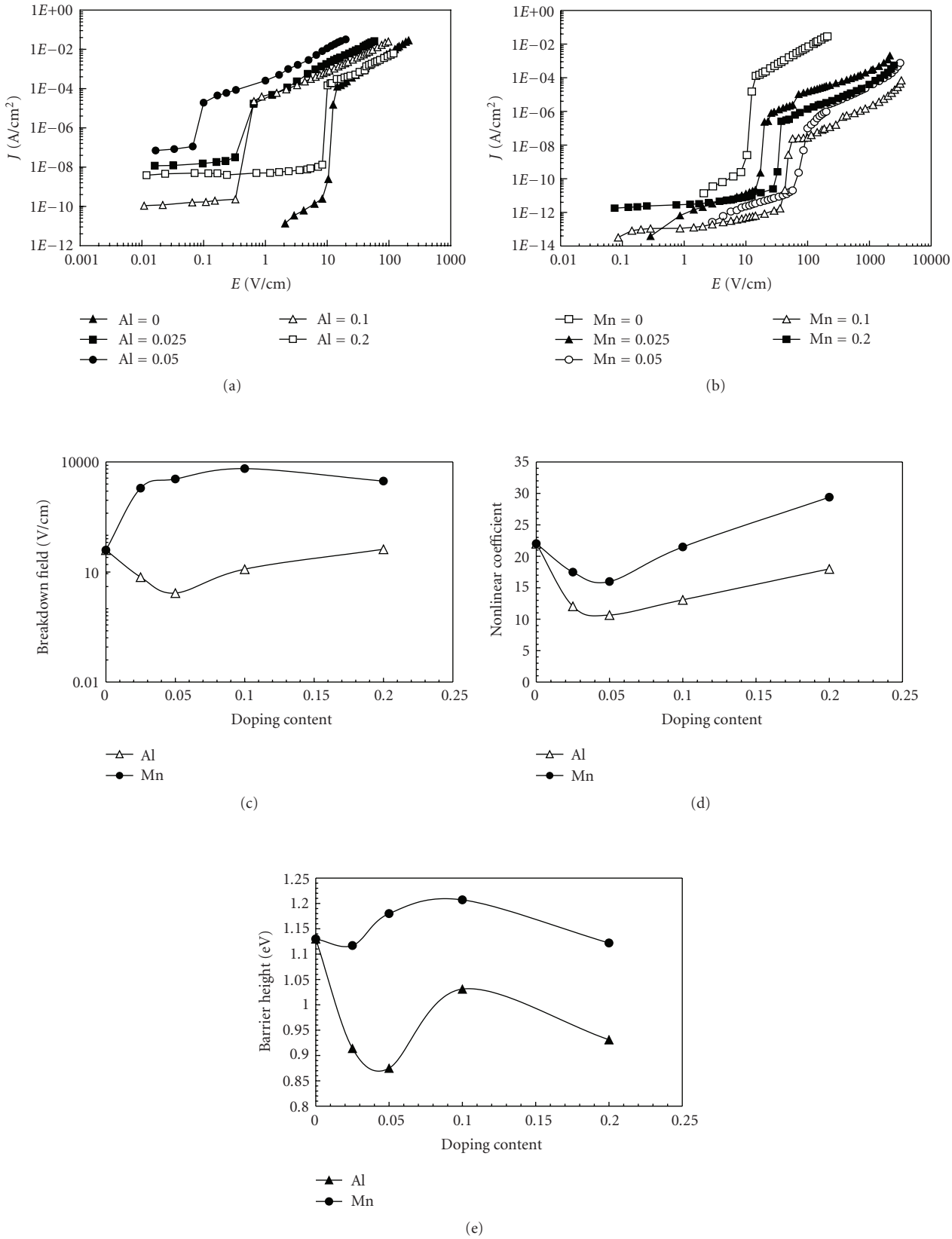

Figure 3: (a) I-V characteristics for Pure and Al doped ZnO samples. (b) I-V characteristics for Pure and Mn doped ZnO samples. (c) Breakdown field for Pure and doped ZnO samples. (d) Nonlinear coefficient for Pure and doped ZnO samples. (e) Barrier height for Pure and doped ZnO samples.

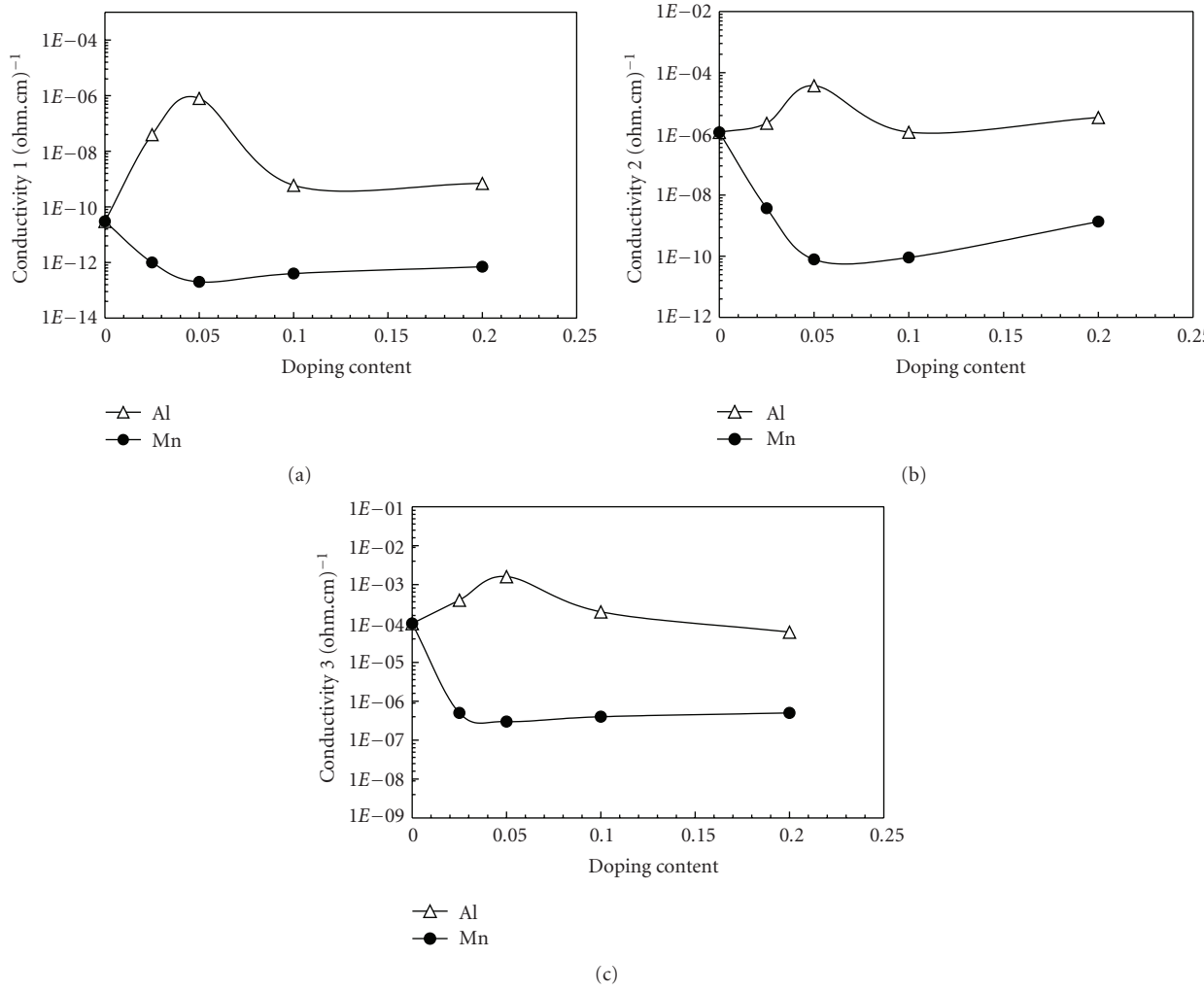

Figure 4: (a) Electrical conductivity across the first region for pure and doped ZnO samples. (b) Electrical conductivity across the nonlinear region for Pure and doped ZnO samples. (c) Electrical conductivity across the third region for Pure and doped ZnO samples.

Since Schottky type grain boundary barriers exist in the present samples, the current density in the ohmic region of varistor is related to the applied electric field by the following formula [13, 17]:

$$J = AT^2 \exp\left[\frac{\beta E^{1/2} - \varphi_B}{kT}\right], \tag{3}$$

where A is Richardson's constant $\{A = (4\rho emK^2/h^3)\}$, ρ is the varistor density, e is the electronic charge, m is the electronic mass, k is the Boltzmann constant, h is Planck's constant, φ_B is the interface barrier height, and β is a constant. By measuring the current density in the ohmic region and keeping the temperature constant, for two different roots of applied fields, the values of φ_B could be obtained. The variation of φ_B against doping content shown in Figure 3(e) indicates that φ_B decreases by Al up to 0.05, followed by an increase at 0.10, and again decreased at 0.20, while φ_B is generally increased by Mn-doping. This behavior is nearly consistent with the behaviors of nonlinear coefficient and breakdown field. These results support the improvements of electrical barriers in the Mn doped samples as compared to both undoped and Al-doped samples.

In ZnO varistors, free electrons can be released and raise the conductivity σ by increasing the density of electron which are considered to be the majority carriers. In the present case, σ is calculated from the (J/E) in the first and third regions (ohmic regions), while, in the second region (nonlinear region), the currents strongly increase due to the decrease of φ_B. Then, the conductivity in the nonlinear region is given by [22]

$$\sigma_2 = \sigma_1 \exp\left\{\frac{(\alpha - 1)(E_2 - E_1)}{E_2}\right\}, \tag{4}$$

where σ_1 is the conductivity in the low field region (first region). E_1 and E_2 are the applied fields across the nonlinear region. Figures 4(a)–4(c) show the dc electrical conductivity as a function of doping content across the three different regions. It is observed that the conductivity, as compared to undoped sample, generally decreases by Mn addition and increased by Al. Anyhow, the conductivity curves shown in

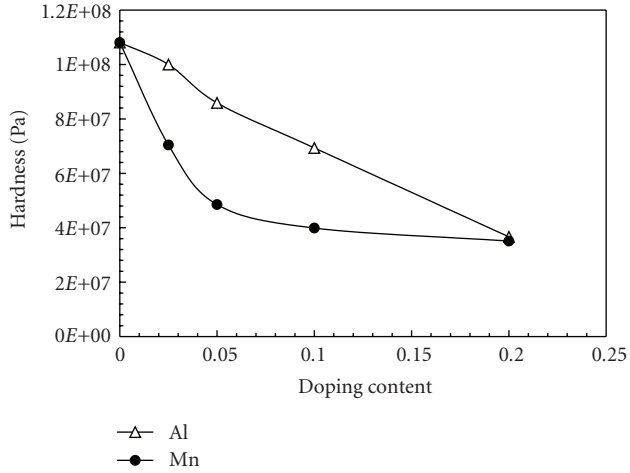

Figure 5: Hardness at 0.98 N for Pure and doped ZnO samples.

Figure 4 could be divided into two regions as follows: the first region at low doping content ($0.00 \leq x \leq 0.05$), in which the conductivity is increased by Al and decreased by Mn; and the second region where ($0.10 \leq x \leq 0.2$), in which the conductivity is nearly unchanged by Al and increased by Mn. But the values of conductivity remain higher for Al than Mn. There are possible factors other than the presence of the second phases, which should be responsible for the reduction of conductivity by Mn doping. This is because these second phases are due to the solubility limit of doping through the ZnO lattice. Therefore, we believe that when Mn is dissolved in ZnO, it behaves as a deep donor and depresses the concentrations of the intrinsic donors at the sintering temperature. When the samples are quenched, the concentrations of these intrinsic donors at room temperature are also lowered. In this way, the conductivity, mainly arising from the ionization of intrinsic donors, is lowered by the presence of low Mn doping content. With increasing Mn content ($0.10 \leq \text{Mn} \leq 0.2$), the solubility limit of Mn through the interstitial position, in which Mn also behaves as an acceptor, exceeds the donor effect and increased the conductivity [23], so, the solubility limit of Mn through Zn lattice is responsible for increasing conductivity at higher content, while the mechanism of Al reaction with Zn in the structure could be described as follows [24, 25].

Neutral Zn interstitial zinc atom is firstly ionized as

$$\begin{aligned} &\text{Zn} \longrightarrow \text{Zn}^{+} + \text{e}, \text{ and secondly ionized as} \\ &\text{Zn}^{+} \longrightarrow + \text{Zn}^{++} + \text{e}. \end{aligned} \tag{5}$$

Such free electrons move to the conduction band of ZnO and enhance the conductivity of ZnO. The conductivity of ZnO can also be increased by extrinsic defects at Zn site such as Al^{3+}. In Zn^{2+} substituted with Al^{3+}, some of free electrons are released and raise the conductivity of ZnO at low values of Al content ($0.00 \leq \text{Al} \leq 0.1$). With increasing Al content ($0.10 \leq \text{Al} \leq 0.2$), the solubility limit of Al through the interstitial position, in which Al also behaves as an acceptor may be equalize the donor effect and keeps the conductivity nearly unchanged.

Figure 5 demonstrates the Vickers microhardness (VHN) plotted as a function of doping content at 0.98 N-applied load. An approximately monotonically linear decrease in VHN with increasing doping content up to 0.20 is observed. This means that the substitution up to 0.20 can substantially suppress microcracking of ZnO ceramics and consequently VHN is decreased. This is probably attributed to weakness of the coupling between the grains and elimination of pores, which may occur by the doping during heat treatments. Then, one can say that the mechanical resistance becomes lower and consequently the mechanical connection is depressed. These results are consistent with SEM photographs where the grains are not close together through the weak link regions. The dark regions between the grains indicate a weak link between them. The question is why the values of VHN for Al remain higher than the values of VHN for Mn. This may be related to the difference in the values of density and grain size between the two dopants.

It is evident from the above results that Al generally leads to break the formation of potential barrier in the grain boundary of ZnO varistor, and consequently both breakdown field and nonlinear coefficient are decreased, While the electrical conductivity is apparently higher than that of the undoped ZnO, indicating that the grain boundary is less resistive than the grains. In contrast, the Mn doping leads to supporting the formation of the potential barrier in the grain boundary, and consequently both breakdown field and nonlinear coefficient are enhanced, whereas the electrical conductivity is apparently lower than that of the undoped ZnO, indicating that the grain boundary is more resistive than the grains. It is well known that Zn^{2+} and Al^{3+} are nonmagnetic ions and Mn is magnetic ion with $4.9\,\mu_B$ magnetic moment. Furthermore, the higher valence state of $Mn^{3+/4+}$ than Al^{3+} may lead to the formation of acceptor levels and make the grain boundary region more resistive. So, we believe that both valence state and magnetic moment of the two considered dopants are responsible for the observed difference in the behaviors of electrical properties between them.

4. Conclusion

A comparative study between effects of Mn and Al on the properties of ZnO varistor is investigated. We have shown that both Mn and Al do not influence the well-known peaks related to wurtzite structure of ZnO ceramics, while, the shape and size of grains and oxygen vacancies are clearly effected by the doping addition and they are different for both dopants. Interestingly, the values of breakdown field, nonlinear coefficient, and barrier height are found to be higher for Mn samples as compared to Al samples, and the opposite, holds for leakage currents, hardness and electrical conductivities. We could increase E_B up to 6571 by 0.10 of Mn addition to ZnO. Furthermore, the Al addition could increase the conductivity up to three times the conductivity of ZnO, and it is approximately (10^3–10^5) times the conductivity of Mn samples. Our results show that the valence state and magnetic moment of the considered

dopants are responsible for the observed difference in the behaviors of electrical properties between them.

References

[1] T. K. Gupta, "Application of zinc oxide varistors," *Journal of the American Ceramic Society*, vol. 73, no. 7, pp. 1817–1840, 1990.

[2] A. B. Glot, "A model of non-Ohmic conduction in ZnO varistors," *Journal of Materials Science: Materials in Electronics*, vol. 17, no. 9, pp. 755–765, 2006.

[3] A. M. R. Senos, M. R. Santos, A. P. Moreira, and J. M. Vieira, "Grain boundary phenomena in the early stages of sintering of MO oxides," in *Surface and Interfaces of Ceramic Materials*, L. C. Dufour, C. Monty, and G. Petot-Ervas, Eds., NATO ASI Series, pp. 553–563, Kluwer Academic, London, UK, 1988.

[4] A. M. R. Senos and J. M. Vieira, "Pore size distribution and particle rearrangement during sintering," in *Proceedings of the 3rd International Conference on Euro-Ceramics*, P. Duran and J. F. Fernandez, Eds., vol. 1, pp. 821–826, Faenza Edit rice Iberica S. L., Faenza, Italy, 1993.

[5] A. M. R. Senos, *Sintering kinetics in open porosity stages of zinc oxide*, Ph.D. thesis, University of Aveiro, Aveiro, Portugal, 1993.

[6] S. Levine, "Theory of varistor electronic properties," *Critical Reviews in Solid State and Materials Sciences*, vol. 5, no. 4, pp. 597–608, 1975.

[7] J. Bwrnasconi, S. Strässler, B. Knecht, H. P. Klein, and A. Menth, "Zinc oxide based varistors: a possible mechanism," *Solid State Communications*, vol. 21, no. 9, pp. 867–870, 1977.

[8] R. Einzinger, "Grain junction properties of ZnO varistors," *Applications of Surface Science*, vol. 3, no. 3, pp. 390–408, 1979.

[9] A. M. R. Senos and J. L. Baptista, "Atmosphere effects in the grain boundary region of ZnO varistors," *Journal of Materials Science Letters*, vol. 3, no. 3, pp. 213–216, 1984.

[10] A. B. Glott, C. A. Hogarth, and R. Bulpett, "Voltage contrast imaging of zinc oxide ceramics," *International Journal of Electronics*, vol. 65, no. 4, pp. 797–804, 1988.

[11] G. D. Mahan, L. M. Levinson, and H. R. Philipp, "Theory of conduction in ZnO varistors," *Journal of Applied Physics*, vol. 50, no. 4, pp. 2799–2812, 1979.

[12] G. E. Pike, "Electonic properites of ZnO varistors: a new model," in *Materials Research Society Symposia Proceedings: Grain Boundaries in Semiconductors*, G. E. Pike, C. H. Seager, and H. J. Leamy, Eds., vol. 5, p. 369, Elsevier, New York, NY, USA, 1982.

[13] A. Sedky, M. Abu-Abdeen, and A. A. Almulhem, "Nonlinear I-V characteristics in doped ZnO based-ceramic varistor," *Physica B*, vol. 388, no. 1-2, pp. 266–273, 2007.

[14] A. Sawalha, M. Abu-Abdeen, and A. Sedky, "Electrical conductivity study in pure and doped ZnO ceramic system," *Physica B*, vol. 404, no. 8–11, pp. 1316–1320, 2009.

[15] M. S. Castro and C. M. Aldao, "Effects of the sintering temperature on the oxygen adsorption in ZnO ceramics," *Journal of the European Ceramic Society*, vol. 19, no. 4, pp. 511–515, 1999.

[16] G. Pei, C. Xia, S. Cao, J. Zhang, F. Wu, and J. Xu, "Synthesis and magnetic properties of Ni-doped zinc oxide powders," *Journal of Magnetism and Magnetic Materials*, vol. 302, no. 2, pp. 340–342, 2006.

[17] V. V. Deshpande, M. M. Patil, and V. Ravi, "Low voltage varistors based on CeO_2," *Ceramics International*, vol. 32, no. 1, pp. 85–87, 2006.

[18] M. Houabes, S. Bernik, C. Talhi, and A. Bui, "The effect of aluminium oxide on the residual voltage of ZnO varistors," *Ceramics International*, vol. 31, no. 6, pp. 783–789, 2005.

[19] M. Matsuoka, "Nonohmic properties of Zinc oxide ceramics," *Japanese Journal of Applied Physics*, vol. 10, no. 6, pp. 736–746, 1971.

[20] J. Han, P. Q. Mantas, and A. M. R. Senos, "Defect chemistry and electrical characteristics of undoped and Mn-doped ZnO," *Journal of the European Ceramic Society*, vol. 22, no. 1, pp. 49–59, 2002.

[21] T. Takemura, M. Kobayashi, Y. Takada, and K. Sato, "Effects of antimony oxide on the characteristics of ZnO varistors," *Journal of the American Ceramic Society*, vol. 70, no. 4, pp. 237–241, 1987.

[22] A. Sedky, under submission to *New Journal of Physics*.

[23] J. Han, P. Q. Mantas, and A. M. R. Senos, "Effect of A1 and Mn doping on the electrical conductivity of ZnO," *Journal of the European Ceramic Society*, vol. 21, no. 10-11, pp. 1883–1886, 2001.

[24] T. K. Gupta, "Microstructural engineering through donor and acceptor doping in the grain and grain boundary of a polycrystalline semiconducting ceramic," *Journal of Materials Research*, vol. 7, no. 12, pp. 3280–3295, 1992.

[25] M. Houabes, S. Bernik, C. Talhi, and A. Bui, "The effect of aluminium oxide on the residual voltage of ZnO varistors," *Ceramics International*, vol. 31, no. 6, pp. 783–789, 2005.